GEOPHYSICS, VOL. 76, NO. 1 (JANUARY-FEBRUARY 2011); P. E9–E20, 9 FIGS., 3 TABLES.
10.1190/1.3511351

PRACTICING GEOPHYSICS

Estimation of elastic moduli of mixed porous clay composites

Erling Hugo Jensen[1], Charlotte Faust Andersen[2], and Tor Arne Johansen[3]

ABSTRACT

We have developed a procedure for estimating the effective elastic properties of various mixtures of smectite and kaolinite over a range of confining pressures, based on the individual effective elastic properties of pure porous smectite and kaolinite. Experimental data for the pure samples are used as input to various rock physics models, and the predictions are compared with experimental data for the mixed samples. We have evaluated three strategies for choosing the initial properties in various rock physics models: (1) input values have the same porosity, (2) input values have the same pressure, and (3) an average of (1) and (2). The best results are obtained when the elastic moduli of the two porous constituents are defined at the same pressure and when their volumetric fractions are adjusted based on different compaction rates with pressure. Furthermore, our strategy makes the modeling results less sensitive to the actual rock physics model. The method can help obtain the elastic properties of mixed unconsolidated clays as a function of mechanical compaction. The more common procedure for estimating effective elastic properties requires knowledge about volume fractions, elastic properties of individual constituents, and geometric details of the composition. However, these data are often uncertain, e.g., large variations in the mineral elastic properties of clays have been reported in the literature, which makes our procedure a viable alternative.

INTRODUCTION

Lithology prediction from seismically derived properties (such as velocity, impedance, and velocity ratio) is important in seismic exploration and reservoir characterization. In siliciclastic rocks, for instance, elastic properties and permeability are known to be strongly influenced by the clay/sand ratio (Castagna et al., 1985; Best and Katsube, 1995). Usually, we need to estimate the so-called effective solid and fluid properties to calculate the impact of lithology and fluid variations on seismic properties. Knowing the effective properties of the solid grains is necessary when, for instance, using the Gassmann equation (Gassmann, 1951) to study pore fluid effects. A common strategy is to use the Hill average (Hill, 1963) to obtain the effective solid properties before applying the Gassmann equation to predict the fluid effects.

In this study, we investigate an alternative approach for modeling the effective properties of mixed clay composites. The basis for the study is a set of experimental data published by Mondol et al. (2007). Here, dry and brine-saturated smectite and kaolinite have been mixed and subsequently subjected to increasing (confining) pressure while P- and S-wave velocities were measured. We consider the mineral heterogeneity not to be on a mineral grain scale (see Figure 1a for illustration of mineral grain scale heterogeneity) but instead to be composed of clusters of each mineral, i.e., as a mixture of porous smectite and porous kaolinite (see Figure 1b). Therefore, we apply the effective elastic properties of the pure samples to define end members, which we then use to study the relevance of various rock physics models without specifying the grain, fluid, or pore properties.

The elastic properties of smectite and kaolinite mineral clusters differ, so we need to take into account the effects of different compaction of the two components, altering the relative volume fractions as pressure is increased. We compare results obtained when the end members are defined at isopressure, at isoporosity, or as an average between these two conditions.

Our approach is somewhat analogous to the one discussed by Gurevich and Carcione (2000) for deriving the elasticity effects resulting from pore fluid alterations in heterogeneous sand/clay mixtures. They propose a composite Gassmann model whereby fluid substitution is performed for each constituent, subsequently using an

Manuscript received by the Editor 9 December 2009; revised manuscript received 23 July 2010; published online 13 January 2011; corrected version published online 19 January 2011.
[1]University of Bergen, Department of Earth Science, Bergen, Norway. E-mail: erling.jensen@geo.uib.no.
[2]On leave from Statoil, Bergen, Norway; presently University of Bergen, Department of Earth Science, Bergen, Norway. E-mail: charlotte.andersen@geo.uib.no.
[3]University of Bergen, Department of Earth Science, Bergen, Norway and NORSAR, Bergen, Norway. E-mail: torarne.johansen@geo.uib.no.

appropriate mixing law to calculate the total effective properties. In our case, we use the experimental data of the effective elastic properties of pure dry and saturated smectite and kaolinite clusters directly in modeling the mixtures.

Our paper is organized as follows. We start by examining the data set of the pure and mixed samples of smectite and kaolinite. Then we define three strategies for selecting pairs of end members from data characterizing the pure samples. For two of the strategies, we specify a correction to the volume fractions of the constituents because of their different compaction. Finally, we examine commonly used rock physics models, with the end members and volume fractions as input, to estimate the elastic properties of the mixed clay composites. We make a statistical comparison between the predicted and measured data for the mixed samples.

DATA SET

We use data from a mechanical compaction experiment reported by Mondol et al. (2007). Six dry and six brine-saturated samples with mixtures of smectite and kaolinite, ranging from 100% smectite to 100% kaolinite in steps of 20% matrix volume fractions, were prepared in the laboratory and exposed to uniaxial (vertical) compression using an oedometer cell. The P- and S-wave velocities and changes in sample heights were measured at pressure intervals of approximately 5 MPa, from 1 to 50 MPa, using the transmission technique (Birch, 1960). Changes in volume were deduced from the measured decrease in the heights of the specimens and were used to compute the porosities and densities. Dynamic bulk and shear moduli were calculated from the velocities and density.

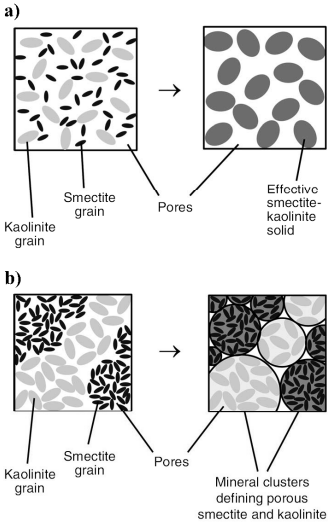

Figure 1. Two ways of modeling the effects of mixed minerals. (a) Homogeneous mixing can be modeled as a composite of single minerals, defining a set of effective (mixed) grain properties. (b) Heterogeneous mixing can be modeled as a composite of mineral clusters, defining effective properties of porous clusters of each mineral.

Figure 2 shows the bulk and shear moduli of the various dry and wet samples measured at 11 different pressures (and porosities), plotted as circles. Because our modeling typically requires input for other porosities or pressures than those which have been measured, we find third-order polynomial fitted functions for these observations and use them to calculate the input values we need.

MODELING APPROACH

The use of effective medium models to obtain the elastic properties of porous composites typically requires knowledge of the corresponding properties of the individual constituents. A general procedure (e.g., Mavko et al., 1998) is first to model the two sets of effective parameters, one for the solid phase and one for the fluid phase, and their respective volume fractions (Figure 1a). Subsequently, the effect of porosity and pore texture is modeled. However, the elastic properties of clay minerals are poorly known and may also depend on the geochemical interaction with the pore fluid (Meade, 1966), which makes the general procedure unsuitable.

We propose an alternative procedure wherein we consider the smectite-kaolinite mixtures to have two phases: one cluster of porous smectite and one cluster of porous kaolinite (Figure 1b). Thus, the effects of mineral and fluid properties, grain geometries, pore space, and structure are embedded implicitly in the effective elastic properties of the two phases. For these properties, we use the measured data of the pure porous smectite and kaolinite samples as end members and input to the effective medium models.

Figure 2 shows that the variation in elastic moduli versus porosity and pressure differs for the pure smectite and kaolinite samples. We will demonstrate how to use these curves to predict the properties of any mixture of smectite and kaolinite.

The mixed samples initially are very loose. As confining pressure increases, the porosity decreases and the bulk and shear moduli increase. We assume that within the pressure range of this experiment (pressure < 50 MPa), the reduction in sample volume is dominated by a reduction of the pore volume; we also assume that alteration of the solid minerals is negligible. The porosity variations seen in Figure 2 should then be a result of mechanical compaction only. The elastic properties of the various mineral mixtures are different, so their compaction rates and porosity reductions are different. As seen in Figure 2c, the porosity in the wet samples reduces with confining pressure from approximately 41% to 11% in the pure kaolinite sample, whereas the range for smectite is 57%–36%. Figure 3 shows schematically the compaction trends and the expected differences in compaction of smectite and kaolinite mineral clusters.

Strategies for selecting modeling end members

To base the modeling on observed data, we avoid using extrapolated values, but we use best-fit values within a porosity range limited by the observations and the approach for selecting end members for the modeling. We consider the following three strategies for defining which end members to use as input to the effective medium models.

Isoporosity

In this strategy, we assume an equal compaction of the pore volumes of the smectite and kaolinite mineral clusters. Hence, both end members and the mixed sample have the same porosity (Figure 4a):

$$\phi_S = \phi_{mix} = \phi_K, \quad (1)$$

where ϕ_S, ϕ_K, and ϕ_{mix} are the porosities in the pure smectite, pure kaolinite, and mixed samples, respectively. Then, in our modeling, the pressures for the pure end members P_S and P_K respectively, and the mixture P_{mix}, are different:

$$P_S \neq P_{mix} \neq P_K \neq P_S. \quad (2)$$

This limits our studied porosity interval to where we have observations for the pure smectite and kaolinite. The porosity values are sampled with a 0.02 increment in the range [0.45, 0.59] for the dry samples and [0.35, 0.41] for the wet samples.

Isopressure

Here, we assume that during compaction the same pressure is applied on the individual clusters in the mixed samples as we observe for the pure samples. Hence, the end members and mixed sample have the same pressure (Figure 4b):

$$P_S = P_{mix} = P_K. \quad (3)$$

However, in our modeling, the porosities are now different:

$$\phi_S \neq \phi_{mix} \neq \phi_K \neq \phi_S. \quad (4)$$

The pressure range is nearly equal for all samples, which gives the largest porosity range of the three approaches. The pressures are calculated from the best-fit function of the pure kaolinite $P_K(\phi)$, with a 0.02 increment in porosity sampling in the range [0.29, 0.59] for the dry samples and [0.11, 0.41] for the wet samples. These pressures are in turn used in the porosity best-fit functions to calculate the porosities of the end members and the mixed samples.

Average

The two previous strategies form extreme bounds in our modeling. The average strategy examines the use of average properties between these two bounds (Figure 4c). In this case, neither the pressure nor the porosity is the same for the end members and the mixed sample:

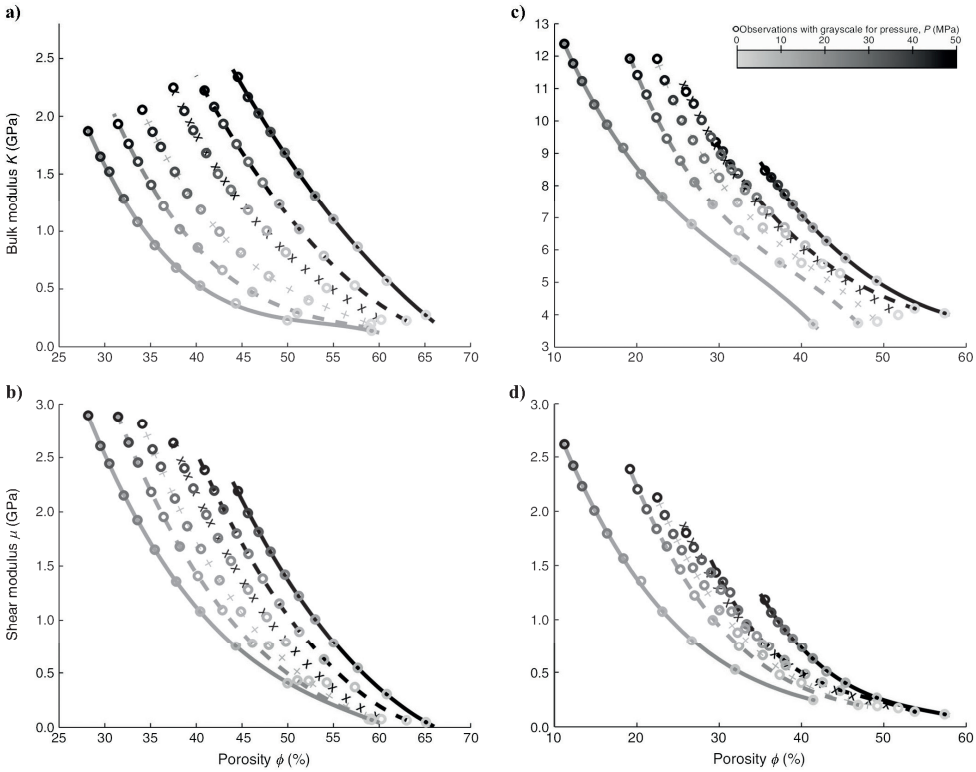

Figure 2. Measured bulk and shear moduli versus porosity for (a, b) dry and (c, d) wet samples. Circles denote moduli calculated from measured P- and S-wave velocities and density. Increased pressure P decreases porosity, as indicated by the gray gradient applied on the circles. Lines are best-fit curves for various smectite-kaolinite mixtures, where S is smectite and K is kaolinite: black solid line (smectite — S100/K0); black dashed line (S80/K20); black x's (S60/K40); gray plus signs (S40/K60); gray dashed line (S20/K80); gray solid line (kaolinite — S0/K100).

$$P_S \neq P_{mix} \neq P_K \neq P_S, \quad (5)$$

$$\phi_S \neq \phi_{mix} \neq \phi_K \neq \phi_S. \quad (6)$$

Porosities in the range [0.37, 0.59] for the dry samples and [0.26, 0.42] for the wet samples are utilized to identify the kaolinite end members and to calculate the corresponding pressure-porosity relation $P_K(\phi)$. Then the average of these porosities and the calculated porosities $\phi(P = P_K)$ for the pure smectite and mixed samples are input into the model.

For the three strategies, the modeling end members are calculated using the obtained porosities as input in the bulk and shear moduli best-fit functions $K(\phi)$ and $\mu(\phi)$, respectively. The porosities and corresponding moduli of the end members can be found in Appendix A.

Volume fraction correction from varying pressure

The initial volume fractions of smectite V_S and kaolinite V_K in the mixed samples refer to the relative matrix fractions. Because we model mixtures of porous smectite and kaolinite, the volume fractions must also capture the relative pore volumes of the constituents. Hence, the volume fraction for smectite L_S is given by

$$L_S = \frac{(\text{smectite mineral volume}) + (\text{smectite pore volume})}{\text{total volume}}. \quad (7)$$

A similar relation can be written for the volume fraction of kaolinite L_K; these fractions must satisfy the equation

$$L_S + L_K = 1. \quad (8)$$

For the isoporosity strategy, we consider the volume fractions of the porous constituents to remain constant and thus resemble the initial volume fractions. For smectite, this means that

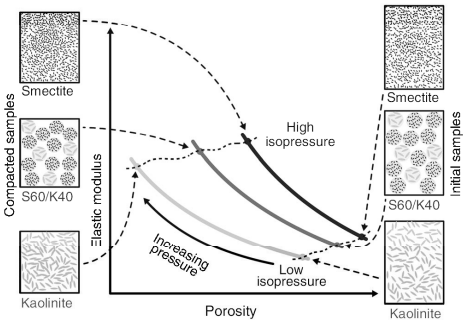

Figure 3. Illustration of how elastic modulus and porosity of pure smectite (black) and kaolinite (light gray) samples with a 60% smectite (S60) and 40% kaolinite (K40) mixture (dark gray) are controlled by confining pressure. The mixture of smectite and kaolinite is illustrated to take place as clusters of the constituents. The pore space of the mineral clusters reduces with increasing compaction, from initial conditions on the right side to final ones on the left side.

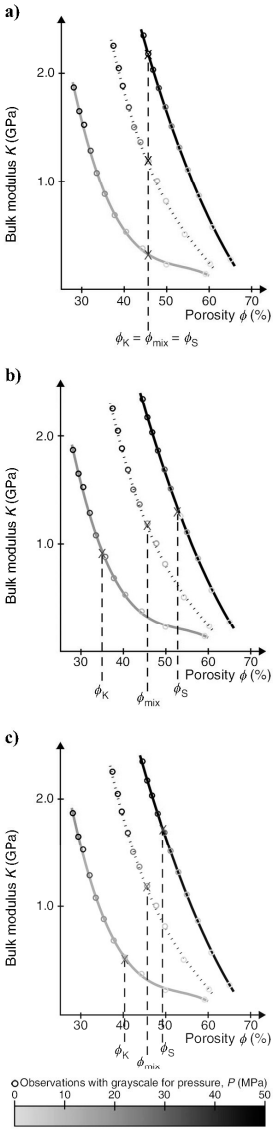

Figure 4. Schematics of the various strategies to model the mixed smectite-kaolinite composites. End members of elastic properties, marked with X, are defined at (a) the same porosity, (b) the same pressure, or (c) the average between (a) and (b). Associated pressures to the measured seismic property are represented in the legend. Black solid line is smectite, dotted line is S40/K40 mixture, and gray line is kaolinite.

$$L_S = V_S. \tag{9}$$

For the isopressure and the average strategies, we perform one set of modeling whereby the volume fractions remain constant, as explained above, and another where the volume fractions change as a result of the relative difference in compaction of the smectite and kaolinite pore space. Then the smectite volume fraction is adjusted by

$$L_S = V_S \frac{1-\phi}{1-\phi_S}, \tag{10}$$

where ϕ and ϕ_S are the porosities that depend on the selected end members of the mixed and pure smectite samples, respectively. (See Appendix B for details about the volume fraction correction.)

Figure 5 shows the predicted porosity effects from compaction given by equation 10 for the isopressure and average strategies, compared with constant volume fractions (equation 9). The largest corrections are clearly seen subsequent to initial compaction; the porosity correction vanishes as the pore space becomes relatively small compared to the total volume.

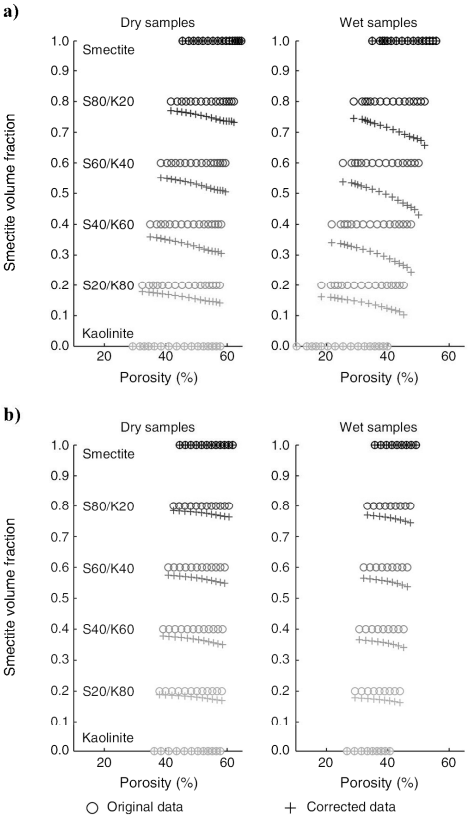

Figure 5. Effect of lithology correction on smectite fraction as a function of porosity when following (a) the isopressure and (b) the average strategy. For the observed porosities the circles denote uncorrected data as given by equation 9 and the crosses denote the corrected data as given by equation 10. The gray gradient refers to the different smectite and kaolinite fractions.

Models used in calculating effective moduli

Eight models are used and compared for predicting the observed elastic moduli of the various mixtures. Reuss (1929), Voigt (1928), Hill (1963), and Hashin-Shtrikman upper and lower bounds (HSUB, HSLB) (Hashin and Shtrikman, 1963) are multipurpose models used for deriving the elastic moduli for any mixture of minerals from the elastic moduli of the individual constituents. Differential effective medium (DEM) modeling (Sheng, 1990) and self-consistent approximation (SCA) (Berryman, 1980a, 1980b) are inclusion-based models that consider the shapes of the inclusions and their respective concentration. Normally, these shapes relate to the shape of the grains or the pore space. But because we model mixing porous clusters of pure smectite and kaolinite, the inclusions in our modeling are not bound by these dependencies. So the spherical inclusions we use do not denote the shape of the individual minerals but the shape of the aggregate of minerals, representing the porous clay constituents.

In the case of DEM, we consider two versions: one where the kaolinite is the host medium (DEM_K) and another where smectite is the host medium (DEM_S). More details of the various models can be found in Appendix C. Predicted bulk modulus versus porosity for these models are shown in Figure 6. The two end members used as input in the modeling are the bulk modulus of the porous material and of the mineral. This is equivalent to considering a plot between two porous materials — one being relatively soft and the other being relatively stiff, where the x-axis denotes volume fractions of the two.

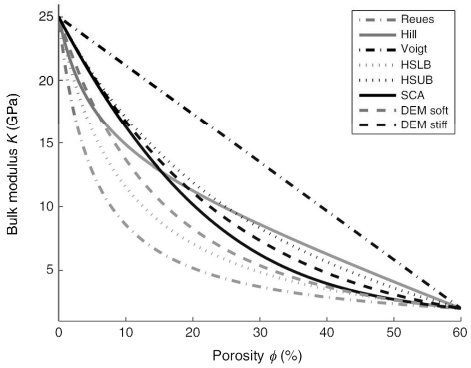

Figure 6. Examples of the estimated bulk modulus as a function of mineral fractions when the difference in bulk modulus of the two constituents (end members) is large. Models: Reuss (dotted-dashed gray curve), Hill (solid gray curve), Voigt (dotted-dashed black curve), Hashin-Shtrikman lower bound (dotted gray curve), Hashin-Shtrikman upper bound (dotted black curve), self-consistent approximation (solid black curve), differential effective medium with the soft material as the host medium (dashed gray curve), and differential effective medium with the stiff material as the host medium (dashed black line).

MODELING RESULTS

To evaluate the results of the modeled versus observed data, we use the rms deviation normalized to the mean of the observed values. This is also referred to as the coefficient of variation of the rms deviation (CVRMSD).

Figure 7 shows the CVRMSD for the bulk and shear moduli, based on isoporosity, isopressure, and average approaches and subsequently used in the eight prediction models. We see that the match between modeled and observed data for the wet samples is better than for the dry samples. The best results for the dry samples have a CVRMSD smaller than 10%, whereas for the wet samples it is less than 5%.

The modeling results generally are more sensitive to the choice of strategy for defining the elastic properties of the end members than the particular rock physics model being used. Thus, isopressure gives a better prediction of the effective elastic properties of the mixed samples than does isoporosity. Of the three approaches, isoporosity implies the largest difference between the elastic properties of the two end members, leading to a stronger rock physics model dependency than for the other two approaches, as revealed in Figure 6. The average gives results almost as good as when considering isopressure.

In general, the volume correction clearly improves the predictions for the isopressure approach. The two exceptions are for modeling the bulk modulus of the dry samples and when applying the Voigt model to calculate the shear modulus of the wet samples. But for the average strategy, this correction only improves the results when the Voigt model is used to calculate the bulk modulus of the dry samples.

Individually, the best results for the bulk and shear moduli of the dry samples are obtained with the Voigt model with end members from the isopressure or average strategy, respectively, both without applying correction to the bulk volume fraction. Overall, the best model to predict both moduli is the HSUB, defining end members by the average strategy and with no volume fraction correction.

The bulk and shear moduli of the wet samples are best predicted

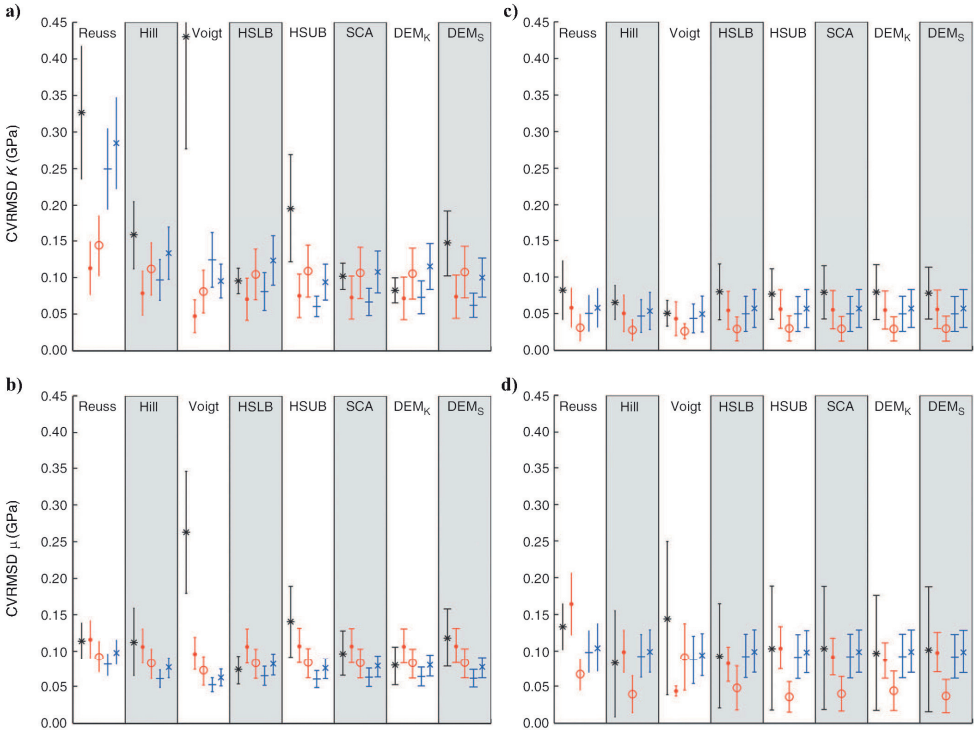

Figure 7. The mean and standard deviation of the coefficient of variation of the rms deviation versus model for the (a) dry bulk modulus, (b) dry shear modulus, (c) wet bulk modulus, and (d) wet shear modulus. The results are grouped for each model: Reuss, Hill, Voigt, Hashin-Shtrikman lower bounds (HSLB), Hashin-Shtrikman upper bounds (HSUB), self-consistent approximation (SCA), differential effective medium with kaolinite as host medium (DEM_K), and differential effective medium with smectite as host medium (DEM_S). The mean values for the various modeling are black asterisk (isoporosity), red dot (isopressure without volume correction), red circle (isopressure with volume correction), blue cross (average strategy without volume correction), and blue asterisk (average strategy with volume correction). The error bars show the standard deviation.

using the isopressure model combined with the volume fraction correction. For the bulk modulus, all effective medium models are almost equally good, but there are some variations in the quality of the shear modulus prediction. Hence, the result for the shear modulus constrains the number of models best suited for a combined modeling of both moduli. Then, all models except for Reuss and Voigt are good candidates, with HSBU being slightly better than the rest.

Examples of effective property predictions

For the wet samples, the HSUB with end members defined as a result of the isopressure strategy gives the best overall modeling predictions for bulk and shear moduli over the entire porosity range and for all lithologies. The modeled data (using HSUB) and measured data of the wet samples are shown in Figure 8. The results are improved when using the volume fraction correction (Figure 8c and d). Ignoring this correction (Figure 8a and b) leads to increasing deviations between modeled and observed data with increasing pressure (i.e., decreasing porosity). In particular, for 20% smectite and 80% kaolinite, HSUB gives a very good prediction when applying the volume correction for the whole porosity range. The prediction of the bulk modulus is improved when one of the clays has a dominant volume fraction; for the shear modulus, the result improves with increasing amount of kaolinite.

DISCUSSION

Poisson's ratio of the wet samples range from 0.40 to 0.49; for the dry samples, there is a large spread between -0.11 and 0.42. In fact, 18 of the 54 values for the dry samples are negative. Auxetic materials, which have negative Poisson's ratios, become thinner perpendicular to the applied force when being compressed. This is not the expected behavior of clay and can be the result of the samples being dried too much — losing some of their chemically bounded water in addition to the pore fluid and thus changing their mineral properties.

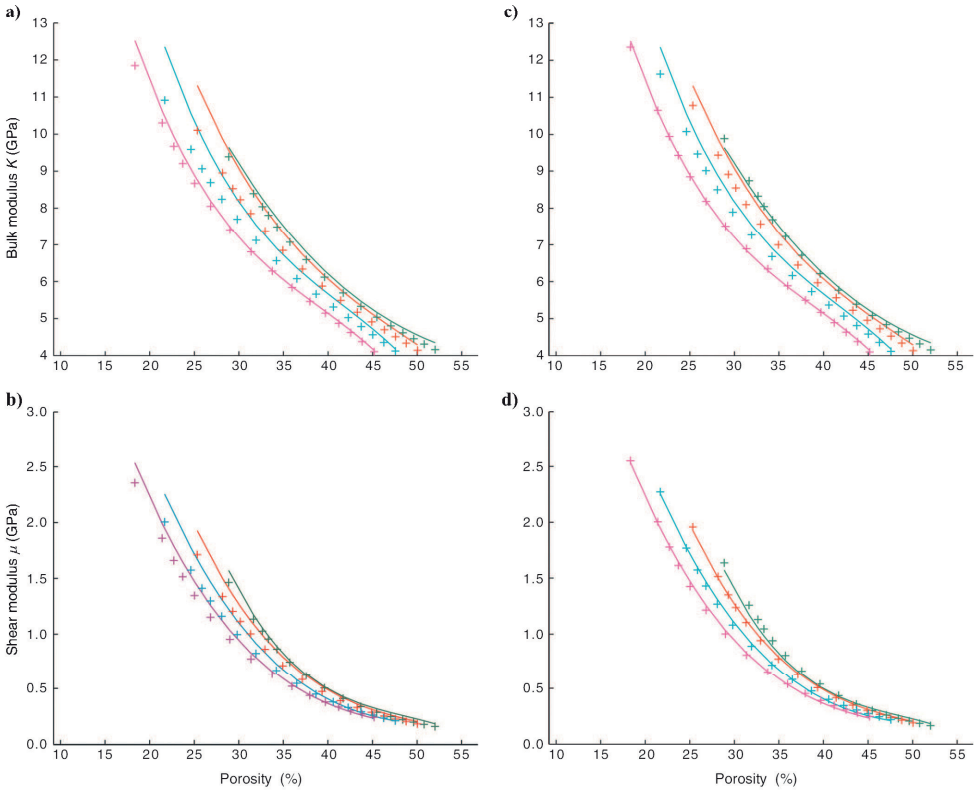

Figure 8. Estimated (a, c) bulk and (b, d) shear moduli for the wet samples using end members of equal pressure. The modeling is done using HSUBs without (a, b) and with (c, d) correction of the bulk volume fraction. Modeled data are plotted as crosses on top of the best-fit curves of the observed data for the various smectite-kaolinite mixtures using the color code: green (S80/K20), red (S60/K40), blue (S40/K60), and purple (S20/K80).

It is unlikely that overdried and wet clay minerals have the same properties. To confirm this, we performed a Gassmann fluid substitution using the observed data from the wet and dry samples of pure smectite and kaolinite to estimate the mineral properties of these two clays; negative bulk moduli values were found for both minerals. Another explanation for the large spread in Poisson's ratio of the dry samples is that there could be some erroneous measurements or specific problems with these samples. Either way, the measurements for the dry samples seem dubious and might be the reason why we have better predictions for the wet samples than the dry ones. This, combined with the fact that most natural clay rocks are water saturated, implies that most attention should be paid to our results for the wet samples.

The strategy for choosing the elastic end members seems to be the most significant factor for the quality of our predictions of the overall elastic moduli. Of the three tested strategies, isopressure and isoporosity are the least and most sensitive to the choice of rock physics models, respectively. This is because the differences in the elastic properties of the end members are smallest when following the isopressure approach and largest for the isoporosity approach. The difference in predicting the bulk modulus for the various models is shown in Figure 6. In the general case, however, the contrast in elastic properties of the mixing minerals might be larger than between smectite and kaolinite. Thus, in those cases, the choice of rock physics model becomes more important for the predicted elastic moduli than in the case of the isopressure approach. But smectite and kaolinite are end members with respect to grain size, surface area, and cation exchange rate (Mondol et al., 2008), and the difference in the elastic moduli of these minerals is expected to be significant — something the measured elastic properties of the two clays at equal porosity supports.

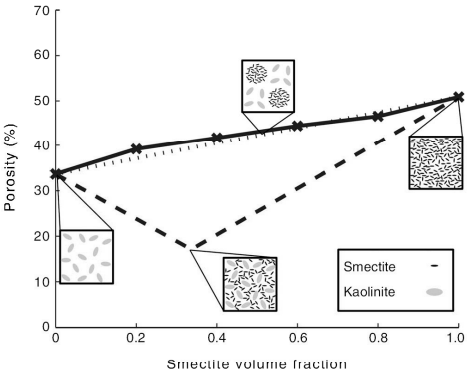

Figure 9. Porosity of mixed smectite-kaolinite sample as a function of volume fraction of porous smectite. A heterogeneous mixed composite (dotted line) will have a linear trend given by the weighted average of the constituents. In the dispersed model (dashed line), the pore space of the large grain-sized mineral (e.g., kaolinite) is filled initially by the small-grain-size mineral (e.g., smectite) (Marion, 1990; Yin, 1992; Dvorkin and Gutierrez, 2002). Plot of the porosity versus volume fraction for the wet sample at confining pressure of 5 MPa (solid line) does not follow the V-shaped trend of the dispersed model.

The isopressure model gives the best result, which is significantly improved when the volume fraction correction is applied. To study pore fluid substitution effects for various pressures, constituents, and rock structure, this correction can be linked to the porosity-distribution parameter of Gurevich and Carcione (2000).

An important assumption in our modeling is that we consider the mixed samples to be composed of clusters of the pure smectite and kaolinite minerals, as illustrated in Figure 1b. If the mixture were more homogeneous, as illustrated in Figure 1a, and because there is such a large difference in volume size of the two clay constituents, it should be possible to observe a V-shaped drop in porosity versus lithology because of the smaller grains filling the pore space of the larger grains (Marion, 1990; Yin, 1992; Dvorkin and Gutierrez, 2002). The trend of a heterogeneous composite mix and the V-shaped trend of a dispersed model are plotted in Figure 9 along with the porosity observations of the wet samples measured at 5 MPa. The observations follow the mixed model and show no V-shaped drop. This supports our assumption that the mixing is not taking place at the grain scale.

The axial (vertical) confining stress will usually cause mineral compaction and some mineral alignment in the horizontal direction, leading to elastic anisotropy. We do not consider this to affect our results seriously, however, because we have limited our analysis to vertical velocities.

CONCLUSIONS

We have demonstrated a procedure for estimating the elastic properties of mixtures of porous smectite and kaolinite from data observations of pure smectite and kaolinite for pressure values between 1 and 50 MPa. We have assumed the mixture constituents to be clusters of pure porous smectite and pure porous kaolinite. Hence, we do not rely the modeling on uncertain estimates of mineral values or pore geometries. Following this procedure, the various rock physics models we have tested show few variations and give almost equally good predictions of the elastic properties. Instead, the dominating factor is the choice of input values (end members) in the modeling.

We have tested three strategies for choosing the pure smectite and pure kaolinite end members: one where they have the same porosity, another where they have the same pressure, and a third that is an average between the other two. We find the best predictions when choosing end members having the same pressure. Furthermore, correcting the volume fractions of the constituents improves the results significantly, showing the importance of taking into account the effect of different compactions of the smectite and kaolinite domains.

The HSUB gives slightly better predictions of the shear modulus for the entire pressure range compared to the other rock physics models. It is therefore the best model to use for these samples of smectite and kaolinite mixtures because the bulk modulus is equally well predicted by all the tested rock physics models.

ACKNOWLEDGMENTS

We thank N. H. Mondol, K. Bjørlykke, J. Jahren, and K. Høeg for providing the data set used in this article. We also thank the Norwegian Research Council (Petromaks program) and Statoil for financial support of the doctoral programs of C. F. Andersen and E. H. Jensen.

APPENDIX A

END MEMBERS USED IN THE MODELING

Tables 1–3 list the porosity, bulk moduli, and shear moduli end members for the various modeling strategies.

APPENDIX B

DERIVATION OF CORRECTION TO THE BULK VOLUME FRACTION

We consider a heterogeneous mixture consisting of clusters of pure porous smectite and kaolinite minerals. One fraction of the pore space can therefore be associated with the smectite and the other with the kaolinite, as observed in Figure 1b. Furthermore, for this experiment, we assume the mineral volume to remain constant during compaction.

The initial smectite volume fraction V_S in the mixed samples only considers the solid phase and is given by

$$V_S = \frac{\text{smectite mineral volume}}{\text{total mineral volume}}. \quad \text{(B-1)}$$

The fraction of smectite mineral to the total volume in the mixed samples $V_{S,\text{mineral}}$ can be expressed as

$$V_{S,\text{mineral}} = V_S(1 - \phi), \quad \text{(B-2)}$$

where ϕ is the total porosity. The smectite volume fraction L_S used in our modeling must also consider the pore space:

$$L_S = \frac{(\text{smectite mineral volume}) + (\text{smectite pore volume})}{\text{total volume}}. \quad \text{(B-3)}$$

If we define $\phi_{S,\text{clusters}}$ as the porosity in the smectite mineral clusters,

$$\phi_{S,\text{clusters}} = \frac{\text{smectite pore volume}}{(\text{smectite mineral volume}) + (\text{smectite pore volume})}, \quad \text{(B-4)}$$

then we can also express $V_{S,\text{mineral}}$ as

$$V_{S,\text{mineral}} = L_S(1 - \phi_{S,\text{clusters}}). \quad \text{(B-5)}$$

Inserting equation B-2 into B-5 and solving for L_S gives

$$L_S = V_S \frac{1 - \phi}{1 - \phi_{S,\text{clusters}}}. \quad \text{(B-6)}$$

For the correction of the bulk volume fraction, we assume that the compaction of the pore space in the mixed samples is the same as for the pure samples. This implies that $\phi_S = \phi_{S,\text{clusters}}$, where ϕ_S is the porosity in the pure smectite sample and equation B-6 becomes equation 10. Observe that if $\phi = \phi_S$, which is always the case for the isoporosity strategy, then equation 10 can be simplified to become equation 9.

Table 1. Porosity, bulk and shear modulus end-member values for the dry and wet samples used in the modeling following the isoporosity approach.

	Smectite end member			Kaolinite end member		
Sample	Porosity (%)	Bulk modulus (GPa)	Shear modulus (GPa)	Porosity (%)	Bulk modulus (GPa)	Shear modulus (GPa)
Dry	45.00	2.268	2.108	45.00	0.3377	0.7005
	47.00	2.007	1.794	47.00	0.2890	0.5713
	49.00	1.761	1.506	49.00	0.2542	0.4600
	51.00	1.528	1.244	51.00	0.2291	0.3638
	53.00	1.310	1.007	53.00	0.2095	0.2800
	55.00	1.106	0.7941	55.00	0.1911	0.2055
	57.00	0.9147	0.6038	57.00	0.1696	0.1377
	59.00	0.7368	0.4356	59.00	0.1409	0.07366
Wet	35.00	8.726	1.238	35.00	5.114	0.4095
	37.00	8.025	1.005	37.00	4.713	0.3490
	39.00	7.387	0.8111	39.00	4.284	0.2978
	41.00	6.809	0.6508	41.00	3.817	0.2539

APPENDIX C

THEORETICAL MIXING MODELS

Voigt, Hill, and Reuss

Voigt (1928) and Reuss (1929) define the upper and lower bounds for the elastic moduli of any isotropic or anisotropic composite. The effective elastic modulus C for a mixture of two constituents with elastic parameters C_1 and C_2 and volume fractions V_1 and V_2 are given by Voigt,

$$C_V = V_1C_1 + V_2C_2, \tag{C-1}$$

and by Reuss,

$$\frac{1}{C_R} = \frac{V_1}{C_1} + \frac{V_2}{C_2}. \tag{C-2}$$

The Hill model (Hill, 1963) is the arithmetic average of the Reuss and Voigt methods, i.e., the elastic modulus is given by

$$C_H = \frac{C_V + C_R}{2}. \tag{C-3}$$

Table 2. Porosity, bulk, and shear modulus end-member values for the dry and wet samples used in the modeling following the isopressure approach.

	Smectite end member			Kaolinite end member		
Sample	Porosity (%)	Bulk modulus (GPa)	Shear modulus (GPa)	Porosity (%)	Bulk modulus (GPa)	Shear modulus (GPa)
Dry	45.46	2.207	2.034	29.21	1.703	2.681
	47.47	1.948	1.725	31.55	1.347	2.250
	49.05	1.754	1.499	32.99	1.161	2.013
	50.56	1.579	1.300	34.44	0.9963	1.795
	52.11	1.405	1.109	36.25	0.8205	1.548
	53.73	1.234	0.9268	38.46	0.6464	1.283
	55.35	1.071	0.7587	40.94	0.4969	1.030
	56.92	0.9218	0.6107	43.53	0.385	0.8088
	58.38	0.7907	0.4857	46.05	0.3102	0.6303
	59.68	0.6795	0.3836	48.38	0.2637	0.4925
	60.80	0.5875	0.3021	50.46	0.2352	0.3885
	61.76	0.5122	0.2379	52.26	0.2164	0.3097
	62.58	0.4505	0.1868	53.81	0.2021	0.2487
	63.29	0.3983	0.1448	55.18	0.1893	0.1991
	63.95	0.3513	0.1081	56.46	0.1759	0.1554
	64.62	0.3051	0.07298	57.77	0.1596	0.1127
Wet	34.92	8.755	1.248	10.23	12.93	2.778
	37.41	7.888	0.9622	13.58	11.12	2.208
	38.31	7.600	0.8742	15.25	10.35	1.960
	38.91	7.415	0.8195	16.62	9.774	1.774
	39.78	7.155	0.7448	18.29	9.141	1.567
	41.08	6.787	0.6451	20.39	8.435	1.335
	42.73	6.355	0.5362	22.82	7.725	1.104
	44.59	5.916	0.4358	25.40	7.073	0.8976
	46.48	5.517	0.3538	27.94	6.507	0.7296
	48.27	5.181	0.2920	30.29	6.027	0.6011
	49.89	4.911	0.2473	32.39	5.619	0.5062
	51.30	4.701	0.2150	34.20	5.270	0.4368
	52.52	4.538	0.1911	35.77	4.963	0.3851
	53.62	4.405	0.1721	37.15	4.681	0.3447
	54.67	4.291	0.1554	38.48	4.399	0.3104
	55.78	4.183	0.1388	39.87	4.086	0.2779

Hashin-Shtrikman bounds

The Hashin-Shtrikman bounds (Hashin and Shtrikman, 1963) are theoretical upper and lower limits of effective moduli of an isotropic mixture. An interpretation of these two bounds is that one of the constituents forms a shell around the other constituent. The upper limit yields a composition where a stiff shell surrounds a soft core, and the lower limit is where a soft shell surrounds a stiff core. For a mixture of two constituents, the upper bound (HSUB) is given by

$$K_{\mathrm{HSUB}} = K_1 + \frac{V_2}{(K_2 - K_1)^{-1} + V_1\left(K_1 + \frac{4}{3}\mu_1\right)^{-1}}, \tag{C-4}$$

$$\mu_{\mathrm{HSUB}} = \mu_1 + \frac{V_2}{(\mu_2 - \mu_1)^{-1} + 2V_1(K_1 + 2\mu_1)\left[5\mu_1\left(K_1 + \frac{4}{3}\mu_1\right)\right]^{-1}}, \tag{C-5}$$

where V, K, and μ are the volume fraction, bulk modulus, and shear modulus, respectively, and where indices 1 and 2 refer to the stiffer and softer materials, respectively. The lower bound (HSLB) is found using the same equations but with index 1 referring to the softer material and index 2 to the stiffer material.

Differential effective medium

In differential effective medium model (Sheng, 1990), one of the constituents acts as the host medium forming the initial background material the other constituents are treated as inclusions. The inclusions of known shape are gradually added into the background material, forming a new background material with new effective elastic properties. This can be realized mathematically using a recursive equation with L iterations; the effective elastic properties of one iteration become input to the next iteration. The total number of iterations must be large enough so that an additional iteration does not change the calculated effective bulk and shear moduli significantly.

We model spherical inclusions and mix only two constituents, so we can use the simplified version of the recursive coupled equations:

$$\frac{K_{n-1} - K_n}{3K_n + 4\mu_{n-1}} = V_n V_2 \frac{K_2 - K_{n-1}}{3K_{n-1} + 4\mu_2}, \tag{C-6}$$

$$\frac{\mu_n - \mu_{n-1}}{\mu_n + F_{n-1}} = V_n V_2 \frac{\mu_{n-1} - \mu_2}{\mu_{n-1} + F_2}, \tag{C-7}$$

Table 3. Porosity, bulk, and shear modulus end-member values for the dry and wet samples used in the modeling following the average approach.

	Smectite end member			Kaolinite end member		
Sample	Porosity (%)	Bulk modulus (GPa)	Shear modulus (GPa)	Porosity (%)	Bulk modulus (GPa)	Shear modulus (GPa)
Dry	44.56	2.328	2.182	36.25	0.8205	1.548
	46.36	2.088	1.891	38.46	0.6464	1.283
	48.18	1.860	1.621	40.94	0.4969	1.030
	49.96	1.647	1.377	43.53	0.3850	0.8088
	51.69	1.452	1.160	46.05	0.3102	0.6303
	53.34	1.275	0.9696	48.38	0.2637	0.4925
	54.90	1.116	0.804	50.46	0.2352	0.3885
	56.38	0.9724	0.6603	52.26	0.2164	0.3097
	57.79	0.8430	0.5350	53.81	0.2021	0.2487
	59.14	0.7244	0.4243	55.18	0.1893	0.1991
	60.47	0.6139	0.3252	56.46	0.1759	0.1554
	61.81	0.5086	0.2348	57.77	0.1596	0.1127
Wet	35.77	8.449	1.144	26.68	6.779	0.8085
	37.70	7.796	0.9337	29.14	6.257	0.6607
	39.55	7.222	0.7637	31.38	5.815	0.5499
	41.31	6.725	0.6289	33.33	5.438	0.4688
	42.97	6.298	0.5225	35.01	5.112	0.4092
	44.54	5.927	0.4381	36.48	4.820	0.3639
	46.07	5.599	0.3698	37.82	4.542	0.3271
	47.6	5.301	0.3133	39.16	4.249	0.2941
	49.20	5.022	0.2652	40.64	3.904	0.2613

$$F_2 = \left(\frac{\mu_2}{6}\right)\frac{9K_2 + 8\mu_2}{K_2 + 2\mu_2}, \tag{C-8}$$

where K_{n-1} is the bulk modulus of the background material, K_n is the effective bulk modulus after adding a volume fraction of V_n of the inclusion material, and μ_{n-1} and μ_n are the background material and effective shear moduli, respectively. The value V_2 is the volume fraction of the inclusion material. The iteration parameter n is given by $n = (2,3,\ldots,L+1)$ and results in index values $(1,2,\ldots,L)$. The host medium acts as the initial background material, identified with index 1 for the first iteration, i.e., $n = 2$. The second constituent acts as the inclusion material and is identified with index 2. The value V_n can be computed from

$$V_n = \frac{V_2}{L - (n-1)V_2}. \tag{C-9}$$

Differential effective medium is an asymmetric model because interchanging the constituents for the host and inclusions will lead to different results.

Self-consistent approximation

In self-consistent approximation (Berryman, 1980a, 1980b), none of the constituents defines a background medium. Instead, inclusions of both constituents are added into a host medium of unknown properties. These unknown properties are perturbed until the effects of the inclusions vanish, at which point these properties represent a unique solution for the effective elastic properties of the mixed material. In practice, this can be done by perturbing the effective elastic properties K^{SCA} and μ^{SCA} until equations C-10 and C-11 are satisfied:

$$\sum_{j=1}^{2}(K_j - K^{SCA})V_j P_j = 0, \tag{C-10}$$

$$\sum_{j=1}^{2}(\mu_j - \mu^{SCA})S_j Q_j = 0, \tag{C-11}$$

where V_j, K_j, and μ_j are the volume fraction, bulk modulus, and shear modulus of inclusion material j, respectively. The values P and Q are geometric factors, which for spherical inclusions are given by

$$P_j = \frac{K^{SCA} + \frac{4}{3}\mu^{SCA}}{K_j + \frac{4}{3}\mu^{SCA}}, \tag{C-12}$$

$$Q_j = \frac{\mu^{SCA} + F^{SCA}}{\mu_j + F^{SCA}}, \tag{C-13}$$

where parameter F is given by equation C-8 (when replacing K_2 and μ_2 with K^{SCA} and μ^{SCA}).

REFERENCES

Berryman, J. G., 1980a, Confirmation of Biot's theory: Applied Physics Letters, **37**, no. 4, 382–384, doi: 10.1063/1.91951.

———, 1980b, Long-wavelength propagation in composite elastic media: Journal of the Acoustical Society of America, **68**, 1809–1831, doi: 10.1121/1.385171.

Best, M. E., and T. J. Katsube, 1995, Shale permeability and its significance on hydrocarbon exploration: The Leading Edge, **14**, no. 3, 165–170, doi: 10.1190/1.1437104.

Birch, F., 1960, The velocity of compressional waves in rocks to 10 kilobars; Part 1: Journal of Geophysical Research, **65**, 1083–1102, doi: 10.1029/JZ065i004p01083.

Castagna, J. P., M. L. Batzle, and T. K. Kan, 1985, Relationships between compressional-wave and shear-wave velocities in clastic silicate rocks: Geophysics, **50**, 571–581, doi: 10.1190/1.1441933.

Dvorkin, J., and M. A. Gutierrez, 2002, Grain sorting, porosity, and elasticity: Petrophysics, **43**, no. 3, 185–196.

Gassmann, F., 1951, Über die Elastizität poröser Medien: Vierteljahrsschrift der Naturforschenden Gesellschaft in Zürich, **96**, 1–23.

Gurevich, B., and J. M. Carcione, 2000, Gassmann modeling of acoustic properties of sand-clay mixtures: Pure and Applied Geophysics, **157**, no. 5, 811–827, doi: 10.1007/PL00001119.

Hashin, Z., and S. Shtrikman, 1963, A variational approach to the theory of the elastic behaviour of multiphase materials: Journal of the Mechanics and Physics of Solids, **11**, no. 2, 127–140, doi: 10.1016/0022-5096(63)90060-7.

Hill, R., 1963, Elastic properties of reinforced solids: Some theoretical principles: Journal of the Mechanics and Physics of Solids, **11**, no. 5, 357–372, doi: 10.1016/0022-5096(63)90036-X.

Marion, D., 1990, Acoustical, mechanical, and transport properties of sediments and granular materials: Ph.D. dissertation, Stanford University.

Mavko, G., T. Mukerji, and J. Dvorkin, 1998, The rock physics handbook: Cambridge University Press.

Meade, R. H., 1966, Factors influencing the early stages of the compaction of clays and sands; review: Journal of Sedimentary Petrology, **36**, 1085–1101.

Mondol, N. H., K. Bjørlykke, J. Jahren, and K. Høeg, 2007, Experimental mechanical compaction of clay mineral aggregates — Changes in physical properties of mudstones during burial: Marine and Petroleum Geology, **24**, no. 5, 289–311, doi: 10.1016/j.marpetgeo.2007.03.006.

Mondol, N. H., J. Jahren, K. Bjørlykke, and I. Brevik, 2008, Elastic properties of clay minerals: The Leading Edge, **27**, 758–770, doi: 10.1190/1.2944163.

Reuss, A., 1929, Berechnung der Fliessgrenze von Mishkristallen auf Grund der Plastizitätbedingung für Einkristalle: Zeitschrift für Angewandte Mathematik und Mechanik, **9**, 49–58, doi: 10.1002/zamm.19290090104.

Sheng, P., 1990, Effective-medium theory of sedimentary rocks: Physical Review B: Condensed Matter and Materials Physics, **41**, 4507–4512, doi: 10.1103/PhysRevB.41.4507.

Voigt, W., 1928, Lehrbuch der Kristallphysik: Teubner.

Yin, H., 1992, Acoustic velocity and attenuation of rocks: Isotropy, intrinsic anisotropy, and stress induced anisotropy: Ph.D. dissertation, Stanford University.